FLOOD HYDRAULICS DUE TO EMERGENT VEGETATION ALONG A RIPARIAN ZONE IN MEANDERING CHANNELS

Zulkiflee Ibrahim[a], Zulhilmi Ismail[a], Sobri Harun[a], Koji Shiono[b], Nazirah Mohd. Zuki[a], Md. Ridzuan Makhtar[a], Mazlin Jumain[a], Mohd. Suhaimi Abd. Rahman[a], Mohamad Hidayat Jamal[a]

[a]Department of Hydraulics and Hydrology, Faculty of Civil Engineering, Universiti Teknologi Malaysia (UTM). 81310 UTM Johor Bahru, Johor, Malaysia
[b]Department of Civil and Building Engineering, Loughborough University, Leicestershire, United Kingdom

Graphical abstract
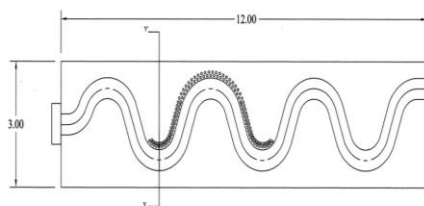
Abstract

Frequent floods around the globe including recent events in several states in Malaysia have damaged the residential properties, infrastructures and crops or even deaths. Clearing vegetations or trees on the floodplain has been pointed out as a contributing factor to the damages. Thus, the influence of floodplain vegetation on the river hydraulics during flooding must be better understood. The hydraulics of flood flows in non-erodible vegetated meandering channel was experimented in the laboratory where two-lined steel rods were installed along a riparian zone to simulate as trees. The stage-discharge relationship, flow resistance, depth-averaged velocity, streamwise vorticity and boundary shear stress patterns during shallow and deep flood inundations were studied. The findings showed that floodplain vegetation had increased the channel flow depth by 32% and its flow resistance. The velocity in vegetated zone was lowered and the shear stress reduced by 86.5% to 91% along the river meander. In addition, the trees also limit flow interaction between main channel and floodplain.

Keywords: Physical modeling; laboratory experiment; meandering channel; floodplain vegetation; flood hydraulics

Abstrak

Kejadian banjir di seluruh dunia termasuklah di beberapa negeri di Malaysia telah memusnahkan harta benda kediaman, infrastruktr, tanam-tanaman dan juga kehilangan nyawa. Penebangan pokok di dataran banjir telah menyumbangkan kepada tahap kemusnahan tersebut. Oleh itu, adalah penting untuk memahami kesan kehadiran pokok-pokok tersebut terhadap hidraulik sungai ketika banjir. Satu kajian makmal ke atas sistem sungai berliku telah dijalankan. Dua barisan rod besi yang digunakan sebagai pokok-pokok telah disusun di atas dataran banjir di sepanjang sungai. Hubungan aras air-kadaralir, rintangan aliran, corak halaju-halaju primer dan sekunder dan tegasan ricih ketika banjir telah dikaji. Hasil kajian telah menunjukkan bahawa kehadiran pokok-pokok tersebut telah meningkatkan kedalaman aliran sebanyak 32% dan juga rintangan aliran. Halaju aliran telah berkurang dan tegasan ricih jugan menurun di antara 86.5% dan 91%. Pokok-pokok juga telah menghadkan aliran di antara saluran utaman dan dataran banjir.

Kata kunci: Permodelan fizikal; eksperimen makmal, saluran berliku, pokok dataran banjir, hidraulik banjir

1.0 INTRODUCTION

Floods have become frequent natural disaster in many part of the world. Disaster statistical data from 1990 to 2014 showed that floods were the highest hazard contributor of 98.7% to Average Annual Loss (AAL) to Malaysia. The floods in Malaysia contributed to 62.5% hazard frequency, 24.1% mortality and 60.0% of economic issues [1]. The recent floods in the states including Kelantan, Pahang, Terengganu, Sabah and Johor have damaged the residential properties, infrastructures, crops and even caused deaths. Deforestation including removal of floodplain vegetation (trees) has been the pointed out as one of the contributing factors to the severity of damages. Therefore, it is essential to understand the influence of floodplain or riparian vegetation on the flooded river hydraulics.

Rivers can be classified as straight, meandering and braiding [2] and meandering is the most common planform acquired by natural rivers. Meandering channel flow is considerably more complex and unique than straight channel. Muar River is the most sinuous Malaysian river in Malaysia with sinuosity of 4.056 while the average sinuosity of Malaysian rivers is about 1.54 [3, 4]. Field work on river hydraulics is difficult partly because compound geometries typically occur under flood conditions when data acquisition is difficult and sometimes dangerous [5]. Among the recent experimental researches on vegetated compound meandering channels flows were Ismail and Shiono [6, 7], Ismail [8] and Jahra *et al.* [9]. The effects of different types of model floodplain vegetation or resistance such as wooden cylinders, vertical rods and even concrete blocks were investigated. However, some existing riparian trees are found to be in too closed spacing between them. Therefore, understanding on the hydraulics of compound or flooded meandering channels with closed-spaced riparian vegetation is still need to be explored.

With regards to the problem, a research was conducted to investigate the flood flow characteristics in non-vegetated and riparian vegetated non-mobile bed compound meandering channels. The research concentrated on stage-discharge relationship, flow resistance, streamwise velocity distribution, horizontal vorticity and boundary shear stress patterns in the channels. The experiment in the physical model was conducted in the Hydraulic Laboratory in Universiti Teknologi Malaysia (UTM). The flood flow characteristics in vegetated and non-vegetated meandering compound channels were studied which involved both shallow and deep flood flow depths in non-erodible meandering channels.

2.0 METHODOLOGY

The experimental research was carried out in a meandering channel constructed in a 12 m long and 3 m wide flume in the Hydraulics Laboratory, UTM. It consisted of main channel and two floodplains on each side. A 0.5 m wide meandering channel with sinuosity of 1.54 was constructed in the flume as illustrated in Figure 1. The channel wave length and meander belt width are 3.4 m and 2.2 m, respectively. The geometrical parameters were main channel width, B_{mc} = 0.5 m and depth, H_{mc} = 0.1 m. The channel was made of rigid boundary type of cross section. The flume bed was set at a gradient of 0.1%. The bed of main channel was filled with uniform graded sand layer and lined with cement to form a non-mobile bed channel. 5 mm diameter steel rods were installed in 2 lined staggered arrays along the right hand side (RHS) riparian zone to simulate as closed spacing emergent floodplain vegetation of 2d where d represented the rod diameter.

A re-circulating flume system in the laboratory was used and discharge was measured using a Portaflo PF 330 flow meter. A point gauge or digital water surface profiler was used to measure flow depth along the main channel while water depth was controlled by two tailgates located at flume downstream. Data measurements were carried out once the difference between water surface and bed slopes was within 5%. This flow state was classified as "quasi-uniform" [10].
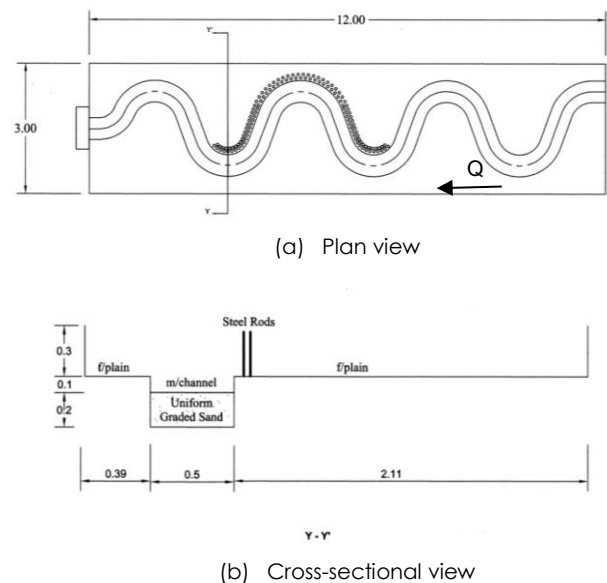

(a)   Plan view

(b)   Cross-sectional view

Figure 1 Two-lined riparian vegetated meandering channel in the experimental study

The three-dimensional velocities were measured using a Nortek Vectrino⁺ Acoustic Doppler Velocimeter (ADV) with a sampling rate of 100 Hz. The minimum recording time for point velocity was one minute. The data collection equipments were placed on a mobile carriageway. Principally, the ADV measures the 3D velocities *(u, v, w)* of water particles located 0.05 m below its probe [11]. The boundary shear stress, τ_b was measured using the Preston tube method, as described in Patel [12], Preston [13] and Sutardi [14].

The measurement sections were located 7 m downstream of channel inlet with a longitudinal distance of half wave length, namely sections S1, S8, and S15 as depicted in Figure 2. The sections S1 and S15 represent the upstream and downstream apices and S8 was the crossover section. The velocities were measured every 0.02 m in transverse direction at several vertical layers.
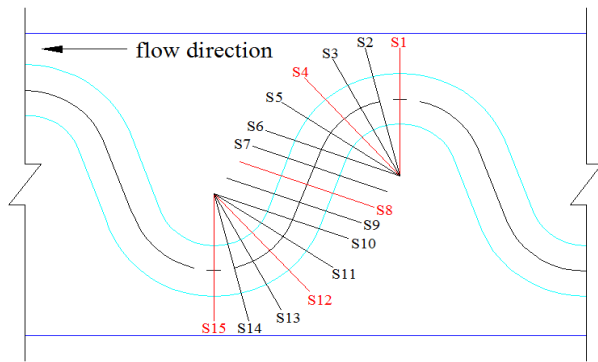

Figure 2 Layout plan of data measurement sections

3.0 RESULTS AND DISCUSSION

3.1 Stage-Discharge

The flooding flow velocities were measured at relative depths or depth ratios *(DR)* of 0.30 (shallow) and 0.45 (deep). The relative depth, *DR* was calculated as given in Equation (1):

$$DR = \frac{(H - H_{mc})}{H} \qquad (1)$$

in which *H* is total flow depth and H_{mc} is the floodplain height (or depth of main channel). The measured maximum velocities recorded at apices sections gave the experimental Reynolds numbers greater than 27,000. Meanwhile, the Froude number ranged from 0.14 to 0.25 which indicated that turbulent subcritical flows took place in the experimental channel.

Figures 3 and 4 depict the stage-discharge and relative depth-discharge relationships for whole section in non-vegetated and riparian vegetated channels. The labels *NV* and *2d* represent non-vegetated floodplain and floodplain with *2d* spacing vegetation, respectively. Meanwhile, d is the diameter of the rigid emergent vegetation. The flow levels in the channel were inbank, bankfull and overbank where bankful

level took place at flow depth of 100 mm. The required discharge to initiate overbank flow in the channel was 17 L/s. As presented in Figure 3, the maximum flow depth for 2d vegetated case increases by 32% compared to non-vegetated case. This is due to the flow retardation effect by the floodplain vegetation of the meandering channel. This effect can also be seen in Figure 4 where the resulted maximum relative flow depths for vegetated and non-vegetated cases are 0.57 and 0.45, respectively.
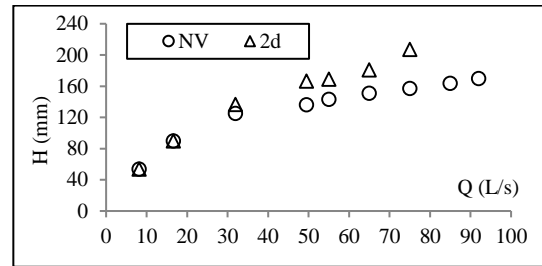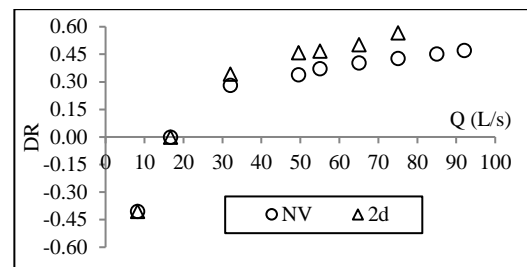

Figure 3 Stage-discharge relationship

Figure 4 Relative depth- discharge relationship

3.2 Manning's Roughness Coefficient

The Manning's roughness coefficient *n* was calculated from stage-discharge data. The usual Manning's equation as shown in Equation (2) was applied to determine the composite Manning's *n* of compound meandering channel.

$$n = \frac{A\,R^{2/3}\,\sqrt{S_o}}{Q} \qquad (2)$$

Figure 5 displays the Manning's *n* for two different cases at various relative depths in the compound meandering channels. The Manning's *n* for non-vegetated increases as flow changes from inbank to overbank. In non-vegetated meandering channel, the roughness value represents the resistance due to the surface of the channel itself. The finding shows that the Manning's *n* increases with relative depth. This also means that *n* increases with discharge in the channels. The *n* values for inbank and bankfull flows are lower as compared to overbank flows values. The Manning's *n* value increases from 0.012 to 0.013 as the flow in meandering channel changes from inbank to bankfull. Subsequently, Manning's *n* value increases as overbank

flow occurs in the channel. The roughness coefficient increases to 0.016 and it is almost uniform for overbank cases which indicates that the main channel and floodplain boundaries increase the flow resistance during flooding. In the case of overbank flow, Manning's n varies and becomes constant as relative depth reaches 0.40. It is common to think that the channel having a single value of n for all occasions.

However, the Manning's n for vegetated cases keep increasing as relative depth increases in the channel. The rod case exhibits the maximum Manning's n value of 0.033 at a relative depth of 0.57. This is a sign of large flow resistance in flooding riparian vegetated meandering channels. In reality the value of n is highly variable and depends on a number of factors including surface roughness, vegetation, channel alignment and channel irregularity [15, 16].
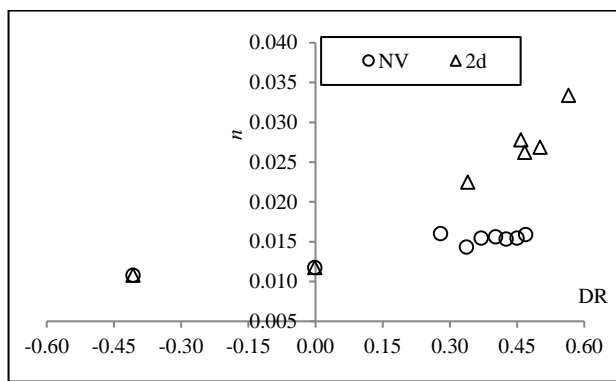

Figure 5 Variations of Manning's n at different relative flow depths

3.3 Primary Velocity Distribution

In order to understand the flow characteristics in a meandering channel, velocity measurements were carried out across sections S1, S8 and S15 (see Figure 2). The 3D velocities (streamwise, transverse and vertical) were measured using the ADV. The method of point velocity measurement has been discussed earlier. The time-averaged velocities were used to plot the spatial distribution across each section. The temporal-averaged velocity components were analysed using the ExploreV software.

The depth-averaged or depth-mean velocity U_d was computed using Equation (3) where the primary or streamwise velocity was averaged over the flow depth. Figures 6 and 7 illustrate the transverse distributions of depth-averaged velocity U_d in compound meandering channels for relative depths of 0.30 and 0.45, respectively.

$$U_{d(y)} = \frac{1}{H(y)} \int_0^{H(y)} U \, dz \qquad (3)$$

The left hand side (LHS) floodplain is located between y = 0 to 20 cm; main channel (MC) is situated between y = 20 to 70 cm and location of right hand side (RHS) floodplain is between y = 70 cm to 90 cm, as illustrated in Figure 6(a). In shallow or low relative flow

depth of 0.30 as presented in Figure 6, it was observed that most of the flow took place in the main channel. Unlike sections S8 and S15, U_d for non-vegetated was larger than vegetated case at section S1, due to that the presence of vegetation on the RHS floodplain which limited flow into floodplain. At the crossover section S8, the vegetation had forced the most of flow to take place in the main channel. No distribution of flow was allowed in the RHS floodplain for vegetated cases which meant that reduction of flow shearing at that section. It can also be seen that the maximum U_d shifts from LHS inner bend at upstream apex S1 to RHS inner bend at downstream apex S15 due to pressure driven secondary flows over water depth. This is opposite to apices inbank flow feature, as mentioned in [17, 18, 19].

Figure 7 shows that when the relative depth rises to 0.45, the flow was distributed more uniform between main channel and floodplains particularly for non-vegetated case. The velocity in RHS floodplain was always small due to the presence of the riparian vegetation or rods. A similar result was observed by Jahra *et al.* [9] where U_d was low in vegetated zone. On the other hand, its magnitude increased as compared to a lower relative depth of 0.30 cases earlier. The U_d in the compound meandering channel for non-vegetated case was always higher than vegetated case at sections S1 to S8. At section S15 values of U_d in main channel and LHS floodplain for vegetated cases increased to almost equal to or higher than U_d values in non-vegetated case because their locations were free from the influence of floodplain riparian rods in the meandering channel. Therefore, water was free to flow at this section, except on the RHS floodplain where the rods were present. Meanwhile the maximum velocities in the vegetated compound meandering channel were 20 cm/s and 35 cm/s during low and high flood water depths respectively. The transverse distribution of depth-averaged velocity showed the presence of shear layers in main channel-floodplain interface zones, which is a common feature in compound channels.
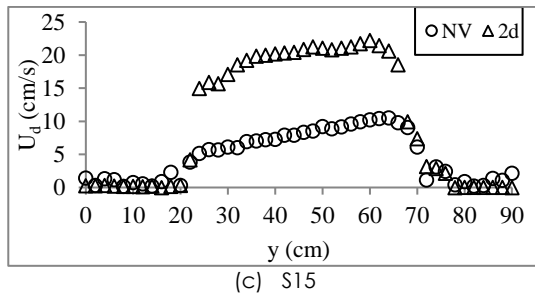

(a) S1

(b) S8

(c) S15
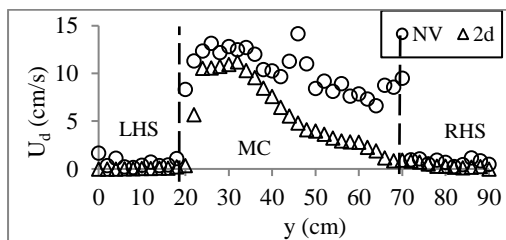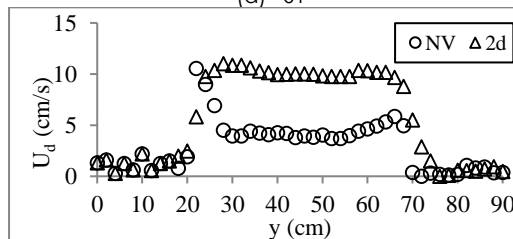
Figure 6 Transverse distribution of depth-averaged velocity, U_d along the meandering channel for low relative depth
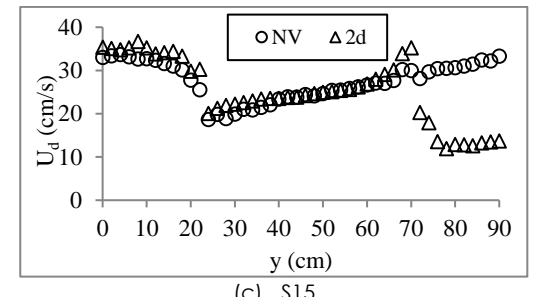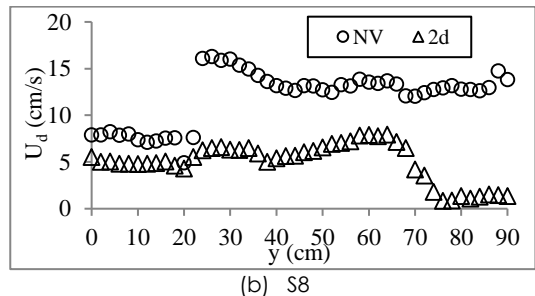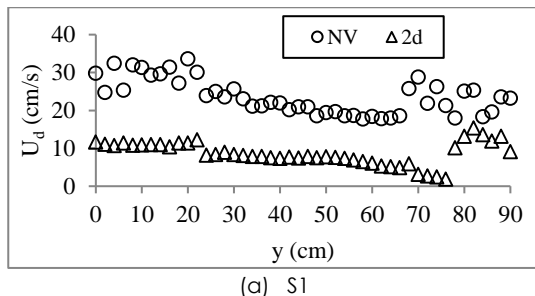

(a) S1

(b) S8

(c) S15

Figure 7 Transverse distribution of depth-averaged velocity U_d along the meandering channel for high relative depth
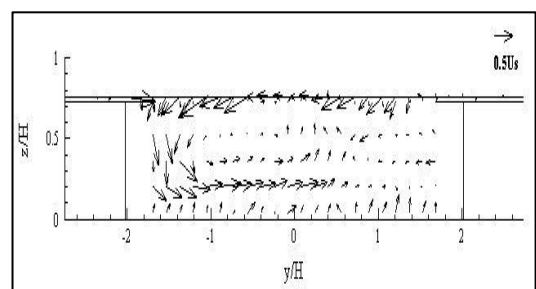
3.4 Streamwise Vorticity

The horizontal secondary flow is also known as circulation or "stream-wise vorticity" [20, 21, 22]. These secondary currents play important roles in river erosion and sedimentation processes. To understand the interaction between floodplain and main channel flows, experimental streamwise vorticity patterns were plotted. Turbulence and centrifugal force in the channel generate the vorticity and its vector Γ is the resultant of measured transverse (v) and vertical (w)

velocities. Figures 8 and 9 present the normalised vorticity patterns at sections S1, S8 and S15 for both shallow and deep flood water depths in the non-vegetated meandering channels. The actual secondary current Γ has been normalised by mean sectional streamwise velocity U_s in the compound channel. Terms y, z and H represent the lateral distance, vertical distance and total flow depth in the channel, respectively.

In shallow flood, the circulation pattern at section S1 in Figure 8 does not clearly show the interaction of main channel and floodplain flows due to low overbank flow depth. The counter-clockwise internal circulation was observed in LHS corner of main channel. Meanwhile, two secondary current cells which indicated the centrifugal force effect as inbank flow, occupied in crossover section S8. A clockwise secondary current cell was observed at LHS corner in the main channel. Contrarily, the flow direction changed at section S15 where clockwise internal flow was seen in the RHS corner of the main channel. In general, the stronger secondary currents occurred in bottom flow layer at apices. The result was similar to Shiono et al. [18] for a non-mobile bed meandering channel. The secondary flow is generated by turbulence and centrifugal force in the channel.

Deep flood flow illustrated in Figure 9 shows stronger secondary currents take place between floodplains and main channel in particular in top flow layers at crossover section S8. This displays the plunging of floodplain flow into main channel and expulsion of main channel flow into floodplain, which was mentioned as flood mechanism in Willetts and Hardwick [23] where turbulence-generated by floodplain flow crossing the main channel is greater than bed-generated turbulence [15]. The results also agreed to Muto and Ishigaki [24] which stated that secondary flow cell became larger as the flood water depth rose, overbank flow structure was controlled by flow interaction at crossover section and secondary flow in main channel was induced by upper layer flow. The internal circulation in counter clockwise direction occurred at the upstream apex section S1, while the opposite direction internal circulation was observed at the downstream apex section S15. This channel bend centrifugal force generated vorticities are also known as Prandtl's first kind secondary currents.
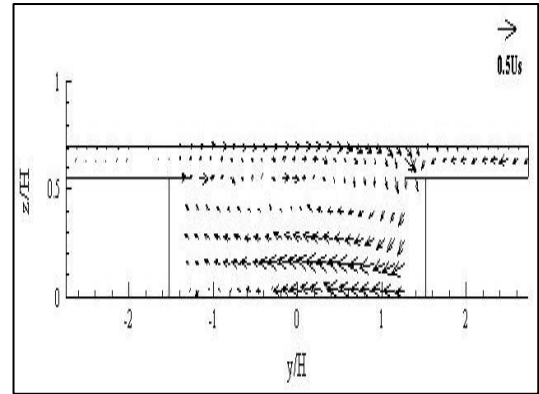

(a) S1
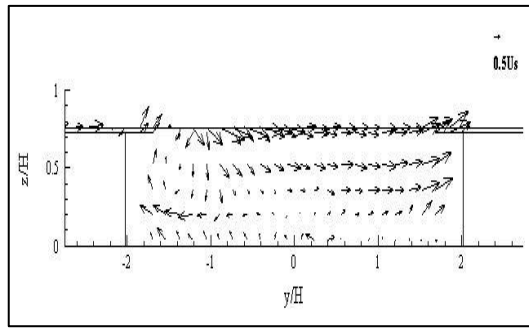
(b) S8
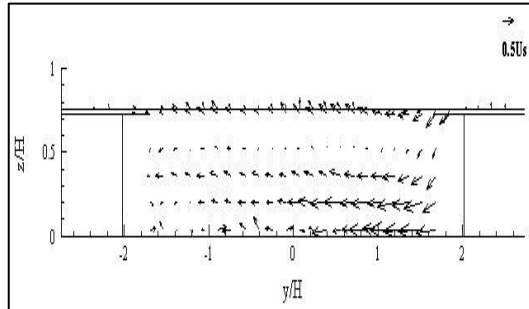
(c) S15

Figure 8 Streamwise vorticity in a non-vegetated meandering channel for relative depth of 0.30
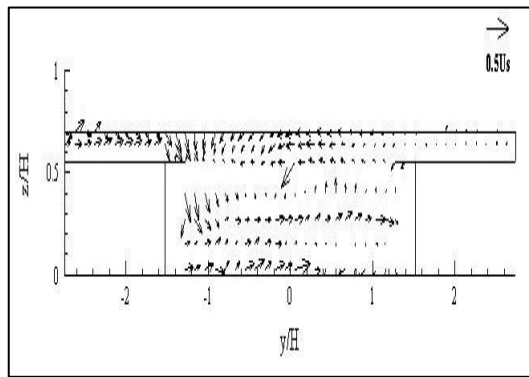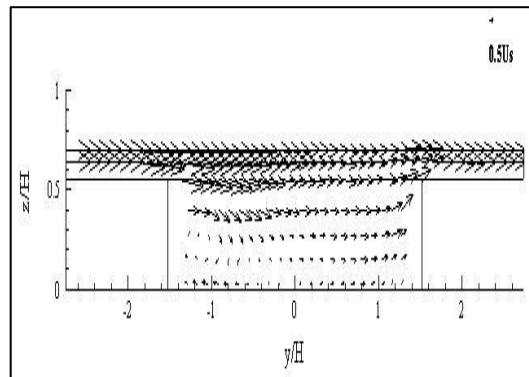

(a) S1

(b) S8

(c) S15

Figure 9 Velocity vectors showing the streamwise vorticity in a non-vegetated meandering channel for relative depth of 0.45

The secondary current patterns for 2d spacing riparian vegetation for low relative depth of 0.30 are displayed in Figure 10. In general, the current patterns are similar to what are shown in Figure 8 in non-vegetated case. However, the riparian vegetation has restricted the main channel flow to enter the RHS floodplain at section S8. Internal circulations are strong at apices S1 and S15 but in opposite directions.

Circulations for a relative depth of 0.45 are depicted in Figure 11. The velocity vectors show that interaction between floodplain and main channel flows becomes stronger and intensified particularly at section S8. Internal vortices start to develop in the mid-depth and bottom flow layer at section S8. Apparently, these internal vortices present in the bottom flow layers at sections S1 and S15, which is a typical apices flow structure. Muto and Ishigaki [24] and Ismail [8] found that vegetation limited and retarded upper flow layer. Meanwhile, Naish and Sellin [25] reported that secondary flow cells became stronger for high flow depth. Thus the experimental results agreed to previous research findings.
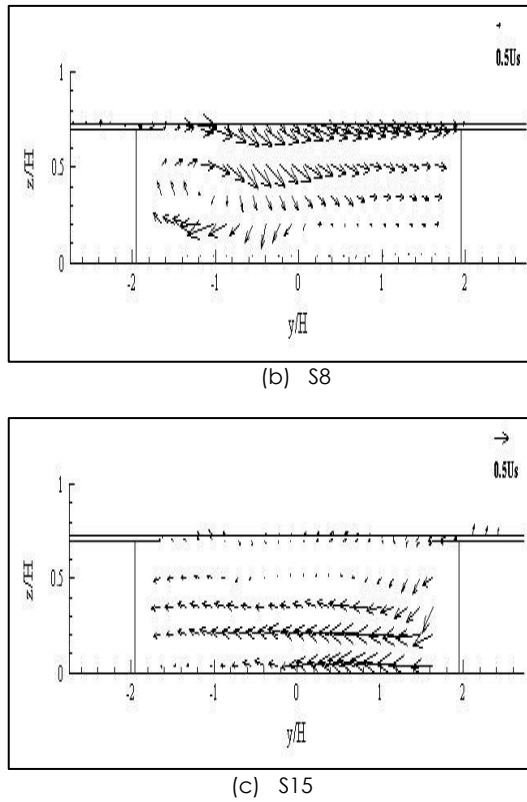

(a) S1

(b) S8

(c) S15
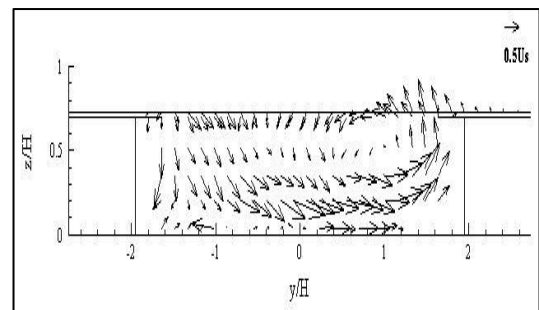
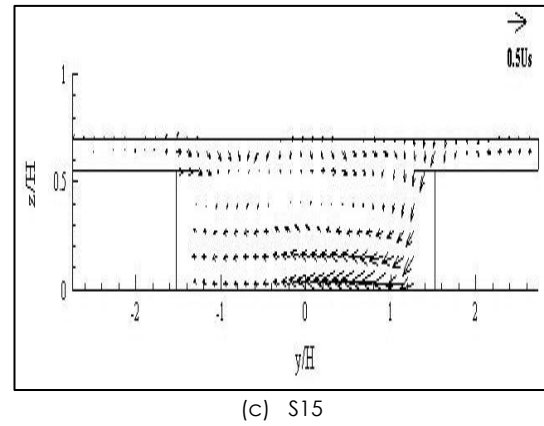**Figure 10** Velocity vectors showing the streamwise vorticity in vegetated meandering channel for relative depth of 0.30

(c) S15

Figure 11 Streamwise vorticity in vegetated meandering channel for relative depth of 0.45

3.5 Boundary Shear Stress

The boundary shear stress τ_b is another important parameter in free surface flow. Figure 12 shows τ_b distributions at sections S1, S8 and S15 for a relative depth of 0.30. The percentage changes of boundary shear stress $\Delta\tau_b$ due to the presence of emergent riparian vegetation were calculated using Equation (4).

$$\Delta\tau_b\ (\%) = \frac{(\tau_{b_{2d}} - \tau_{b_{NV}})}{\tau_{b_{NV}}} x\ 100 \qquad (4)$$

In which τb_{2d} and τb_{NV} are vegetated and non-vegetated shear stresses, respectively.

It is well understood that the velocity influences the τ_b distribution in the main channel. The maximum τ_b at section S1 is 0.21 N/m^2 for non-vegetated case. The drag force induced by the rods reduces the maximum τ_b by 77.8% in the 2d vegetated case. As the water travelled downstream to crossover section S8, the boundary shear stress was lowered; the maximum τ_b in main channel for vegetation case decreased by 83.0% as compared to non-vegetated case. Further reduction of boundary shear stress was observed at downstream section S15. Table 1 summaries the analysis on the measured boundary shear stress in the meandering channel during low flood at a relative depth of 0.30.
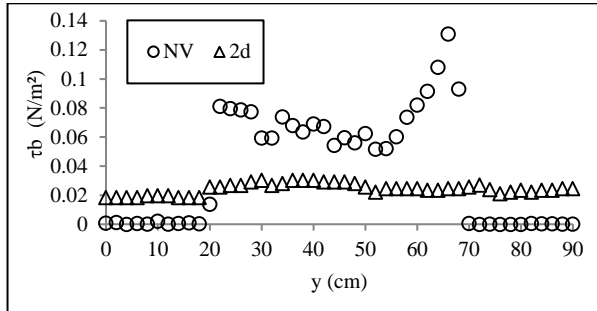
Table 1 Maximum τ_b analysis in main channel for low relative depth of 0.30

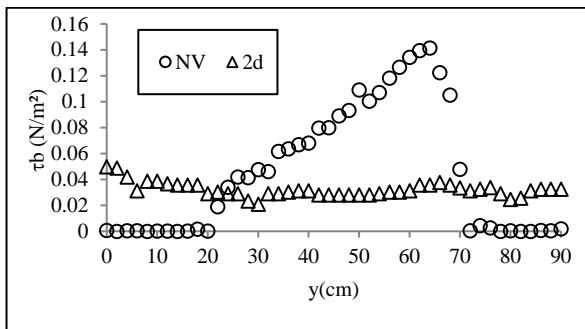| Section	$T_{b\ (NV)}$ (N/m^2)	$T_{b\ (2d)}$ (N/m^2)	$\Delta\tau_b$ (%)
S1	0.21	0.05	-77.8
S8	0.13	0.02	-83.0
S15	0.14	0.03	-81.8

(a) S1

(b) S8
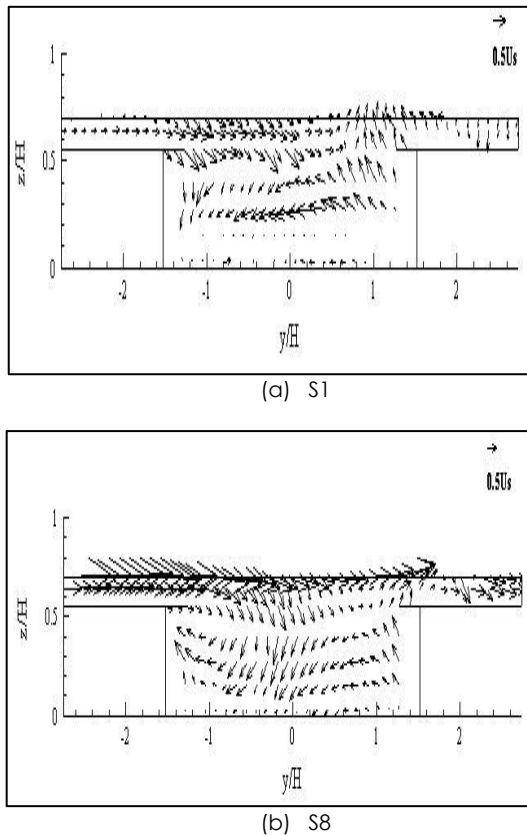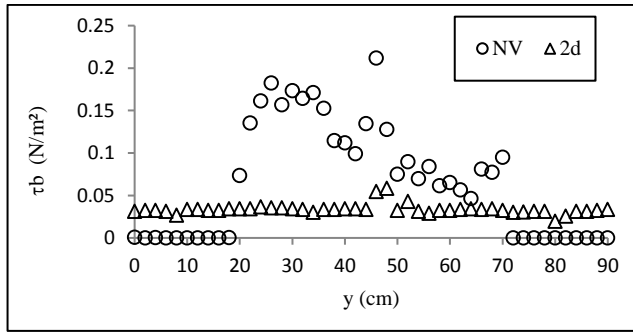
(a) S1

(b) S8

(c) S15

Figure 12 Boundary shear stress distributions for low relative depth of 0.30

Meanwhile, Figure 13 illustrates the boundary shear stress τ_b distributions at sections S1 to S15 for high relative depth of 0.45. The boundary shear stress increased as the relative depth rose from 0.30 to 0.45 mainly due to the growing of velocity in the main channel. The maximum τ_b at section S1 increased to 0.41 N/m² for non-vegetated case. However the rods drag force reduced the maximum τ_b by 91.0% in the vegetated case. As the water moved downstream to crossover section S8, the boundary shear stress was lowered; the maximum τ_b in the main channel was 0.22 N/m² for non-vegetated and it declined in 2d vegetation case by 86.5%. However, the shear stress rose slightly at downstream apex section S15 due to the local velocity increased in the section. Table 2 summaries the shear stress analysis in the main channel of the meandering channel during high flood level of 0.45. It is apparent

that maximum boundary shear stress occurs in the maximum velocity zone. The results have shown that vegetation has lowered the boundary shear stress in the meandering channel. On the whole, the results for both relative depths of 0.30 and 0.45 agreed to findings by Ismail [8] and Sun *et al.* [26] where the emergent vegetation lowered the velocity and boundary shear stress in vegetated zones. The spatial distribution of boundary shear stress followed the velocity distribution across the compound meandering channels.

Table 2 Maximum shear stress τ_b analysis in main channel for deep relative depth of 0.45

Section	$\tau_{b\,(NV)}$ (N/m²)	$\tau_{b\,(2d)}$ (N/m²)	$\Delta\tau_b$ (%)
S1	0.41	0.04	-91.0
S8	0.22	0.03	-86.5
S15	0.45	0.04	-91.6
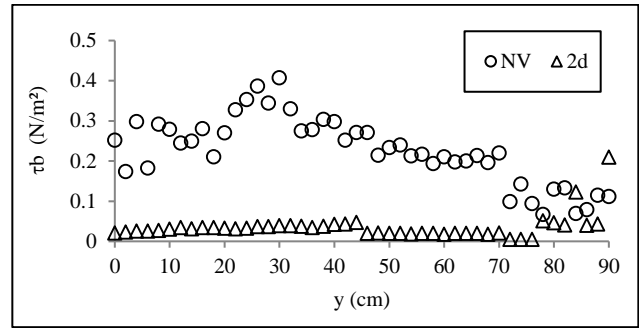
(a) S1
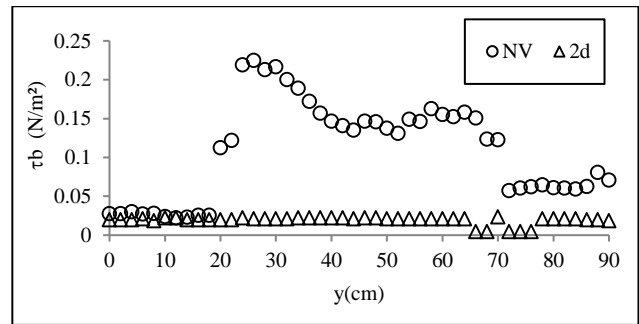
(b) S8
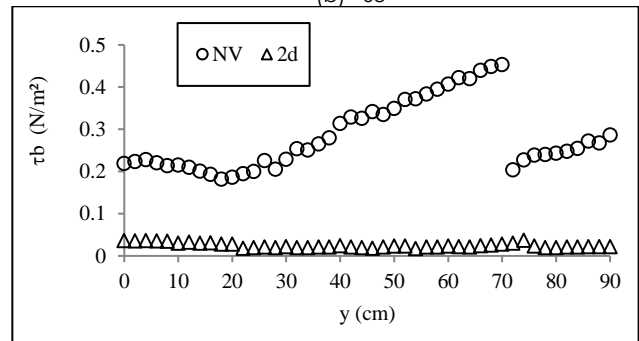
(c) S15

Figure 13 Distributions of boundary shear stress for high relative depth of 0.45

4.0 CONCLUSION

The hydraulics of riparian vegetated and non-vegetated non-mobile bed meandering channels for shallow and deep overbank flows had been investigated through flume simulations. The findings of the experimental study are: (i) riparian vegetation increase flood flow depth in main channel due to flow retardation effect, (ii) riparian vegetation also increases the channel flow resistance and resulted larger Manning's *n* in deeper flood flow, (iii) depth-averaged velocity distributions are influenced by riparian vegetation and relative flow depth. The velocity patterns are also varied along the meandering channel, (iv) turbulence and centrifugal force-generated secondary flows are observed in the meandering channel and strong main channel-floodplain flows interaction takes place in the crossover section during high flood, and (v) the results for both relative depths show that the emergent riparian vegetation lowered the velocity and boundary shear stress in vegetated zones. The spatial distribution of boundary shear stress is influenced by the streamwise velocity across the compound channel.

Acknowledgement

References

[1]   United Nation Office for Disaster Reduction (UNISDR). 2014. Malaysia: Disaster and Risk Profile. www.preventionweb.net/countries/mys/data.

[2]   Leopold, L.B. and M.G. Wolman. 1957. *River Channel Patterns: Braided, Meandering and Straight.* U.S. Geological Survey Professional Paper 282-B. 39-85.

[3]   Ibrahim, Z., Z. Ismail, S. Harun, N.M. Kalimuddin, M.R. Makhtar, and T.N.T. Yunus. 2012. Flood Flow Characteristics in Non-Vegetated Meandering Channel: A Flume Simulation. *Proc. International Conference on Water Resources (ICWR 2012),* Langkawi. 5-6 November 2012. 31-39.

[4]   Ibrahim, Z. 2015. *Flow Behaviour Due to Floodplain Roughness Along Riparian Zone in Compound Channels.* Universiti Teknologi Malaysia. PhD Thesis.

[5]   Myers, W.R.C., D.W. Knight, J.F. Lyness, J.B. Cassells, and F. Brown. 1999. Resistance Coefficients for Inbank and Overbank Flows. *Proc. Instn. Wat. Marit. & Energy,* 136(6): 105-115.

[6]   Ismail, Z. and K. Shiono. 2006. The Effect of Vegetation Along Cross-Over Floodplain Edges on Stage-Discharge, Sediment Transport Rates in Compound Meandering Channels. *Proc.* of 5th WSEAS Int. Conf. on Env. Ecosystem & Development. Venice. 407-412.

[7]   Ismail, Z. and K. Shiono. 2007. The Behaviour of Stage-Discharge, Flow Resistance and Sediment Transport Influenced by Floodplain Roughness. *5th Int. Symp. on Environmental Hydraulics, Arizona, USA.* CD ROM.

[8]   Ismail, Z. 2007. *A Study of Overbank Flows in Non-Vegetated and Vegetated Floodplains in Compound Meandering Channels.* Ph.D Thesis, Loughborough University, U.K.

[9]   Jahra, F., H. Yamamoto, R. Tsubaki, and Y. Kawahara. 2010. Turbulent Flow Structure in Meandering Vegetated Open Channel. *River Flow 2010.* 153-161.

[10] Sun, X. and K. Shiono. 2009. Flow Resistance of One-Line Emergent Vegetation Along the Floodplain Edge of a Compound Open Channel. *Journal in Advances Water Resources.* 32(3): 430-438.

[11] Nortek AS. 2004. *Vectrino Velocimeter User Guide.*

[12] Patel, V.C. 1965. Calibration of Preston Tube and Limitations on Its Use in Pressure Gradients. *Journal Fluid Mech.* 23: 185-208.

[13] Preston, J.H. 1954. The Determination of Turbulent Skin Friction by Means of Pitot Tubes. *Journal of the Royal Aeronautical Society.* 14: 109-121.

[14] Sutardi 2003. Preston Tube Measurement: The Simplest Method to Estimate Wall Shear Stress. *Jurnal Teknik Mesin.* 3(2): 31-38.

[15] Chow, V.T. 1959. *Open Channel Hydraulics.* Singapore: McGraw-Hill.

[16] Sturm, T.W. 2001. *Open Channel Hydraulics.* Singapore: McGraw Hill.

[17] Willetts, B.B. and P. Rameshwaran. 1996. Meandering Overbank Flow Structures. In Ashworth, Bennett, Best and McLelland (eds.). *Coherent Flow Structures in Open Channel.* New York: John Wiley and Sons. 609-629.

[18] Shiono, K., J. Spooner, T. Chan, P. Rameshwaran, and J. H. Chandler. 2008. Flow Characteristics in Meandering Channels with Non-Mobile and Mobile Beds for Overbank Flows. *Journal of Hydraulic Research.* 46(1): 113-132.

[19] Ismail, Z., Z. Ibrahim, and S. Harun. 2011. Inbank and Overbank Flows Characteristics in a Non-Vegetated Meandering Channel. *Proc. Seminar Penyelidikan Kejuruteraan Awam (SEPKA 2011) UTM Johor Bahru.* 13-15 September 2011. 114-119.

[20] Tang, X. and D.W. Knight. 2009. Analytical Models for Velocity Distributions in Open Channel Flows. *Journal of Hydraulic Research.* 47(4): 418-428.

[21] Sanjou, M. and I. Nezu. 2009. *Turbulence Structure and Coherent Motion in Meandering Compound Open Channel Flows. Journal of Hydraulic Research.* 47(5): 598-610.

[22] Tominaga, A. and I. Nezu. 1991. Turbulent Structure in Compound Open Channels. *Journal of Hydraulic Engineering.* 117(1): 21-41.

[23] Willetts, B.B. and R.I. Hardwick. 1993. Stage Dependency for Overbank Flow in Meandering Channels. *Proc. Instn. Civ. Engrs. Wat. Marit. & Energy.* 101(3): 45-54.

[24] Muto, Y. and T. Ishigaki. 1999. Secondary Flow in Compound Sinuous/Meandering Channels. In Rodi, W. and D. Laurence, D. (eds.) *Engineering Turbulence Modelling and Experiments –4.* Elsevier Science Ltd. 511-520.

[25] Naish, C. and R.H.J. Sellin. 1996. Flow Structure in a Large-Scale Model of a Doubly Meandering Compound River Channel. In Ashworth, Bennett, Best and McLelland (Eds.). *Coherent Flow Structures in Open Channel.* New York: John Wiley and Sons. 631-654.

[26] Sun, X., K. Shiono, P. Rameshwaren, and J.H. Chandler. 2010. Modelling Vegetation Effects in Irregular Meandering River. *Journal of Hydraulic Research.* 48(6): 775-783.